Image Cover Sheet

CLASSIFICATION	SYSTEM NUMBER
UNCLASSIFIED	155034

TITLE

SEA SURFACE MODELING & SIMULATION

System Number:

Patron Number:

Requester:

Notes:

DSIS Use only:

Deliver to: FF

National Defence / Défense nationale

SEA SURFACE MODELING & SIMULATION

by

Anastasios Drosopoulos

DEFENCE RESEARCH ESTABLISHMENT OTTAWA
REPORT NO. 1282

Canada

December 1995
Ottawa

National Defence
Défense nationale

SEA SURFACE MODELING & SIMULATION

by

Anastasios Drosopoulos
Surveillance Radar Group
Airborne Radar and Navigation Section

DEFENCE RESEARCH ESTABLISHMENT OTTAWA
REPORT NO. 1282

PCN
03C03

December 1995
Ottawa

Abstract

This report describes the modeling and generation of realistic sea surfaces using directional wave number spectra. Model details are explained and a preliminary investigation into nonlinear, non-Gaussian aspects is carried out. The surfaces so generated can be used as input in current radar scattering models to accurately predict sea clutter behavior.

Résumé

Le présent rapport décrit la modélisation et la création de surfaces de mer réalistes à l'aide de techniques de spectres directionnels du nombre d'ondes. Les particularités du modéle sont expliquées. Le rapport comprend également une étude préliminaire des aspects non-linéaires et non-gaussiens. Les surfaces créées peuvent fournir des données pour des modèles actuels de diffusion radar afin de prévoir, avec précision, le comportement de fouillis de mer.

Executive Summary

This report describes a framework for modeling and generating realistic sea surfaces using directional wave number spectra. The surfaces so generated can be used as input into current radar scattering models to predict sea clutter behavior more accurately. The final goal of this work is to improve small target detection in a sea clutter environment.

There are basically two possible ways of characterizing sea clutter. Radar engineers normally take the practical approach, where empirical distributions of sea clutter are estimated, under typical radar operating conditions, with a certain category of radars. These "custom" distributions are then used to estimate radar detection performance.

The other approach is to look into the physics of the actual electromagnetic scattering mechanism from the sea surface. In the microwave frequency regime, where radar operates, this is a very complicated problem as the number of factors that affect the return signal can be prohibitively large and difficult to adequately model. The common route is to make simplifying approximations which do not always lead to agreement with experimental observations.

As part of the latter approach, work is underway at DREO to build a scattering model that describes all the radar significant aspects of microwave scattering from the sea surface. The first step in this task is to build an accurate model of the sea surface, that can subsequently be used as input to the scattering model. This report describes the necessary framework for this task.

Starting from basic principles, the linear, Gaussian component of the sea surface is described and the need for accurately determining the actual sea surface wavenumber directional spectrum is pointed out. The description of the sea surface with a simple scalar such as "sea state" is no longer sufficient. Statistics and model parameters are outlined and some nonlinear, non-Gaussian aspects are investigated. Finally, a comparison with field data is made that illuminates the difference between theory and practice.

The most important observation from the work presented, is, that a model of the sea surface in equilibrium is not adequate for the typical case of a non fully developed sea. It appears that for radar detection of small targets in sea clutter, there should be an operational mode that estimates the current sea surface spectrum and utilizes this estimate in a way that optimizes target detection. Work is underway in developing such an architecture.

Contents

Abstract iii

Executive Summary v

List of Tables ix

List of Figures xii

1 Introduction 1

2 Background 3

3 Linear Modeling 5

3.1 Digital Filtering 5

3.2 Linear Superposition 6

3.3 Directional Ocean Spectra Examples 7

3.3.1 Pierson-Moskowitz Realization 8

3.3.2 Trunk's Superposition Model 14

3.3.3 The Donelan-Pierson Model 15

3.3.4 The Fung and Chen Empirical Spectrum 18

4 Non-Linear Modeling 20

5 MARCOT Spectra 25

6 Conclusion 27

References 28

List of Tables

1 Wind speed and ΔK resolution based on the spatial resolution Δx and the grid size N. Spatial resolution values examined are $\Delta x = 0.1$ m (L-band) and $\Delta x = 0.01$ m (X-band). 10

List of Figures

1 The Pierson-Moskowitz non-directional wavenumber spectrum for $u_{10} = 2$, 5, 10 and 15 m/s on the left, and the directional spectrum for $u_{10} = 10$ m/s on the right. 10

2 Three surface patches and their histograms based on the Pierson-Moskowitz spectrum. The generating program uses a fixed $N = 512$ and takes as input the patch size L, wind speed u_{10} and wind direction θ_w. From top to bottom: (a) $L = 100$ m, $u_{10} = 4$ m/s, $\theta_w = 0°$, (b) $L = 100$ m, $u_{10} = 15$ m/s, $\theta_w = 0°$, (c) $L = 1000$ m, $u_{10} = 10$ m/s, $\theta_w = 45°$. The image histograms are compared with the Gaussian pdf. 11

3 Correlations in the x and y directions of the three cases in Fig. 2. Solid line is x direction, dashed line is y. The wind direction is $\theta_w = 0°$ for the first two graphs and $\theta_w = 45°$ for the third. 12

4 A Trunk surface realization. The surface plot on the left and the grayscale image of the same surface patch on the right. 14

5 The Donelan-Pierson non-directional wavenumber spectrum for $u_{10} = 2$, 5, 10 and 15 m/s on the left, and the directional spectrum for $u_{10} = 10$ m/s on the right. 15

6 Three surface patches and their histograms based on the Donelan-Pierson spectrum. The generating program uses a fixed $N = 512$ and takes as input the patch size L, wind speed u_{10} and wind direction θ_w. From top to bottom: (a) $L = 100$ m, $u_{10} = 4$ m/s, $\theta_w = 0°$, (b) $L = 100$ m, $u_{10} = 15$ m/s, $\theta_w = 0°$, (c) $L = 1000$ m, $u_{10} = 10$ m/s, $\theta_w = 45°$. The image histograms are compared with the Gaussian pdf. 16

7 Correlations in the x and y directions of the three cases in Fig. 6. Solid line is x direction, dashed line is y. 17

8 The Fung and Chen empirical spectrum. A surface patch 100×100 m^2, the histogram and the correlations in the x and y directions. 19

9 Tayfun's narrow-band nonlinear model for a 1.5×1.5 km patch, the histogram and the correlations in the x and y directions. Note the significant departure from Gaussianity in the histogram. 24

10 Some of the MARCOT spectra. Top left was at 7:45, top right at 7:50, middle left at 7:55, middle right at 8:00 and bottom one at 8:05. The variability in time and developing bimodality is clearly evident. 26

1 Introduction

The advent of high-resolution radars has introduced new problems in the area of target detection in sea clutter. The expectation was that with the smaller sea surface area intercepted by the narrower radar pulse, the sea clutter would be less, leading to a significant detection improvement. Indeed, the number of scatterers per resolution cell is less, however, the central limit theorem no longer applies and the high-resolution sea clutter statistics are no longer Gaussian. This has the effect of introducing target-like "spikes" in the radar return signal that raise the level of false alarms and make small target detection more difficult.

A better understanding of sea clutter is therefore required, in order to properly take it into account in radar detection system design considerations. There are basically two possible ways of characterizing sea clutter. Radar engineers normally take the practical approach, where empirical distributions of sea clutter are estimated, under typical radar operating conditions, with a certain category of radars. These "custom" distributions are then used to estimate general radar detection performance.

The other approach is to look into the physics of the actual electromagnetic scattering mechanism from the sea surface. In the microwave frequency regime, where radar operates, this is a very complicated problem as the number of factors that affect the return signal can be prohibitively large and difficult to adequately model. These are system and environment factors, such as wind speed and direction, pressure, temperature and salinity of the marine environment (air and sea interface), wave geometry and dynamics, radar frequency, polarization, and antenna and receiver characteristics. The common route is to make simplifying approximations which do not always lead to agreement with experimental observations.

For both approaches, the practical and the theoretical, a considerable amount of model validation with well truthed, real data, is a necessary requirement.

Recent advances in computing capabilities now make possible the construction of more "complete" physical models of microwave scattering from the sea surface. Work is therefore underway at DREO to build a scattering model that describes all the radar significant aspects of this phenomenon. The first step in this task is to build an accurate picture of the sea surface (hydrodynamics), that can subsequently be used as input to the scattering model (electromagnetics). This report describes the framework for such a sea surface modeling/generation process.

The sea surface boundary is described by a set of non-linear hydrodynamic equations. The common procedure used to solve these equations is to linearize them using the theory of small departures about some equilibrium condition. The original random models of gravity waves were based on such a linearization and the assumption of Gaussianity seemed to work "well enough" with the experimental data of the time.

The next two sections follow this approach, focusing mostly on implementation aspects. Starting from basic principles, the linear, Gaussian component of the sea surface is described and the framework is outlined of how to use the actual sea surface wave directional spectrum to generate realistic sea surface samples. The common description of the sea surface with a scalar such as "sea state" simply gives a rough idea of the size of the sea waves involved. The wave directional spectrum, on the other hand, gives a clear quantified picture of the distribution, size and direction of sea waves. As such, it can be more useful. Its use is definitely appreciated by companies building off-shore structures in the sea. Ordinary marine radars can be, and are, used as sensors to extract this spectrum. It is time to use this capability and devise methods to take this spectrum into account to improve radar detection performance in a marine environment.

Despite its success, the linear, Gaussian model has its shortcomings and a number of scientists, over the past fifty years, have attempted to tackle some of the nonlinear aspects. A brief overview of this is given in the nonlinear section of this report, and a simple nonlinear implementation of a narrow band sea is carried out. Finally, spectra from ground-truthed data collected during the MARCOT trials (June 95) are presented, illuminating the difference between a fully-developed sea at equilibrium (the common case in sea model development) and a realistic and more typical case of a developing sea (currently an active and challenging research area).

The report ends with a summary of conclusions and areas of future work that can improve this sea surface modeling.

2 Background

The sea surface is the result of a large number of surface waves, mostly wind generated, as well as being generated through nonlinear wave-wave interactions. Ignoring the nonlinear interactions and assuming that for practical purposes the water is infinitely deep, Kinsman [7, pg. 385] claims that the sea wave system, over an area of perhaps 500 miles on a side, can be represented as a particular realization of a quasi-stationary Gaussian process, completely characterized in a statistical sense by the sea surface spectrum. Other workers limit this area to 5-10 square kilometers.

This viewpoint is the simplest to implement in sea surface modeling since the theory of Gaussian stochastic processes is well developed. The sea surface elevation is written as a function of position and time,

$$\zeta(x, y, t) = \zeta(\mathbf{x}, t)$$

with covariance function

$$C(\mathbf{x}, t) = \mathsf{E}\left\{[\zeta(\mathbf{x}_0, t_0) - m(\mathbf{x}_0, t_0)][\zeta(\mathbf{x}_0 + \mathbf{x}, t_0 + t) - m(\mathbf{x}_0 + \mathbf{x}, t_0 + t)]\right\}$$

where m is the process mean and $\mathbf{x}$ is the vector representation of (x, y). It is usually convenient to measure the displacements, ζ, from the mean free surface level so that the mean function is set to $m(\mathbf{x}, t) = 0$. The sea surface directional wavenumber-frequency spectrum is defined as the Fourier transform of [10] $C(\mathbf{x}, t)$,

$$S(\mathbf{K}, \omega) = \frac{1}{(2\pi)^3} \int_{-\infty}^{\infty} \int_{-\infty}^{\infty} \int_{-\infty}^{\infty} C(\mathbf{x}, t) e^{-j(\mathbf{K}\cdot\mathbf{x} - \omega t)} d\mathbf{x} dt$$

where $d\mathbf{x}$ is a shorthand notation for $dxdy$, with

$$C(\mathbf{x}, t) = \int_{-\infty}^{\infty} \int_{-\infty}^{\infty} \int_{-\infty}^{\infty} S(\mathbf{K}, \omega) e^{j(\mathbf{K}\cdot\mathbf{x} - \omega t)} d\mathbf{K} d\omega$$

its inverse, where

$$\mathbf{K} = (K\cos\theta, K\sin\theta) = (K_x, K_y)$$

is the wavevector, K is the wavenumber, θ is the angle the direction of wave propagation makes with the x-axis and ω is the angular frequency of the waves in radians per second.

The spectrum can also be defined in terms of the Fourier components of the surface displacement itself. Assuming that $\zeta(\mathbf{x}, t)$ is a stationary random function of both position and time, it can be represented as a Fourier-Stieltjes integral [10]

$$\zeta(\mathbf{x}, t) = \int_{\mathbf{K}} \int_{\omega} dA(\mathbf{K}, \omega) \exp\{j(\mathbf{K}\cdot\mathbf{x} - \omega t)\}$$

over all $\mathbf{K}, \omega$ space, where $dA(\mathbf{K}, \omega)$ is the Fourier-Stieltjes coefficient. In terms of these Fourier-Stieltjes coefficients,

$$\mathsf{E}[dA(\mathbf{K}, \omega) dA^*(\mathbf{K}', \omega')] = \begin{cases} 0 & \text{if} \quad \mathbf{K}, \omega \neq \mathbf{K}', \omega' \\ S(\mathbf{K}, \omega) d\mathbf{K} d\omega & \text{if} \quad \mathbf{K} = \mathbf{K}', \omega = \omega' \end{cases} .$$

The fact that they are uncorrelated is entirely a consequence of homogeneity and stationarity; it does not imply independence. For a stationary and homogeneous wave field, the spectrum $S(\mathbf{K},\omega)$ is real and positive for all $\mathbf{K},\omega$.

The directional wavenumber spectrum is given by

$$\Psi(\mathbf{K}) = \int_{-\infty}^{\infty} S(\mathbf{K},\omega)d\omega$$

and the frequency spectrum by

$$\hat{\Phi}(\omega) = \int_{-\infty}^{\infty}\int_{-\infty}^{\infty} S(\mathbf{K},\omega)d\mathbf{K} \quad .$$

$\hat{\Phi}(\omega)$ is real and symmetric about $\omega = 0$ so it is usually convenient to regard frequency as positive and define the frequency spectrum as

$$\Phi(\omega) = \begin{cases} 2\hat{\Phi}(\omega) & \text{for} \quad \omega \geq 0 \\ 0 & \text{for} \quad \omega < 0 \end{cases} \quad .$$

Finally, the frequency-directional spectrum is defined as

$$F(\omega,\theta) = \int_{-\infty}^{\infty} S(\mathbf{K},\omega)KdK$$

and the surface height variance is given by

$$\sigma^2 = \int_{-\infty}^{\infty}\int_{-\infty}^{\infty}\int_{-\infty}^{\infty} S(\mathbf{K},\omega)d\mathbf{K}d\omega = \int_0^{\infty} \Phi(\omega)d\omega \quad .$$

One way to interpret $S(\mathbf{K},\omega)$ is as the density of contributions to σ^2 per unit volume of wavenumber-frequency space. Similarly, $\Phi(\omega)$, as the density of contributions to σ^2 per unit frequency interval regardless of the wavenumber magnitude or direction. More simply, wavenumber and frequency spectra of the sea surface characterize the second order spatial and temporal properties of the surface.

Most sea surface elevation measurements are taken from a fixed point. Therefore, the frequency spectrum is the one that is usually obtained. Since electromagnetic wave and sea surface wave interactions are wavenumber dependent, the wavenumber spectrum is the one required. The relation between the two is through the dispersion equation, which, to 4th order, is given by [2]

$$\omega^2 = gK\left(1 + \frac{K^2}{K_m^2} + \frac{5}{4}\frac{K^4}{K_m^4}\right)$$

where $K_m^2 = g\rho/\tau$, g is the gravitational constant, ρ is the sea water density and τ is the water surface tension.

The dispersion equation is important since it encapsulates the linear and non-linear components of how a sea surface wave system evolves in time. When nonlinear effects are not considered, and for deep water environments, the linear term is usually considered sufficient.

3 Linear Modeling

An outline, with examples, is given of how to generate sea surface patches based on the wave directional spectrum. The development here focuses on two-dimensional images, but can easily be extended to three dimensions.

3.1 Digital Filtering

Digital filtering is a standard linear signal processing method which generates stochastic processes with desired properties. A zero-mean Gaussian white noise image, $g(i,j)$, is taken as input and passed through a filter, $w(i,j)$, resulting in the output, $\zeta(i,j)$:

$$\zeta(i,j) = (w \star g)(i,j) = \sum_{n=1}^{N} \sum_{m=1}^{M} w(n,m) g(i-n, j-m) \quad . \tag{1}$$

The autocorrelation of the output is given by

$$C(u,v) = \mathsf{E}\left\{ \left[\sum_n \sum_m w(n,m) g(i-n, j-m) \right] \left[\sum_k \sum_\ell w(k,\ell) g(i+u-k, j+v-\ell) \right] \right\} =$$

$$= \sum_n \sum_m \sum_k \sum_\ell w(n,m) w(k,\ell) \mathsf{E}\left[g(i-n, j-m) g(i+u-k, j+v-\ell) \right] =$$

$$= \sum_k \sum_\ell w(k,\ell) w(k-u, \ell-v)$$

since

$$\mathsf{E}[g(i,j) g(n,m)] = \delta(i-n, j-m) \quad .$$

From standard properties of two-dimensional Fourier transforms, for a real output $\zeta(i,j)$ the filter should be centro-symmetric, i.e.

$$C(i,j) = \sum_k \sum_\ell w(k,\ell) w(k-i, \ell-j) = \sum_k \sum_\ell w(k,\ell) w(i-k, j-\ell) \quad .$$

Taking the Fourier transform of the above equation we have

$$S(k,\ell) = |W(k,\ell)|^2 \quad ,$$

where $S(k,\ell)$ is the surface spectrum. Therefore, the filter weights can be obtained through

$$w(i,j) = \mathcal{F}^{-1}\{\sqrt{S(k,\ell)}\} \quad , \tag{2}$$

and the surface $\zeta(i,j)$ can be generated in the space domain through equation (1), or, through an intermediate step in the frequency/wavenumber domain:

$$Z(k,\ell) = W(k,\ell) G(k,\ell) \quad \Rightarrow \quad \zeta(i,j) = \mathcal{F}^{-1}\left\{ \sqrt{S(k,\ell)} G(k,\ell) \right\} \quad . \tag{3}$$

Note that $G(k,\ell) = |G(k,\ell)| \exp(j\phi_{k\ell})$, with $|G(k,\ell)| = 1$ if we take the Gaussian image to have variance $\sigma_g^2 = 1$.

In order to simulate a surface patch using a model that is determined from a measured or theoretical sea surface spectrum, the step-by-step implementation is:

1. Generate a Gaussian white noise image $g(i,j)$ and compute its Fourier transform $G(k,\ell)$.
2. Take the given $S(k,\ell)$ and form the product $\sqrt{S(k,\ell)}G(k,\ell)$.
3. Compute the inverse FFT of the above product. This gives the surface patch $\zeta(i,j)$.

3.2 Linear Superposition

Another approach, valid to first order perturbation, is that of adding together a number of sinusoidal waves with random amplitudes, phases, directions and frequencies:

$$\zeta(x,y,t) = \sum_{n=1}^{N} \sum_{m=1}^{M} a_{nm} \cos \psi_{nm}$$

where

$$\psi_{nm} = K_{xn}x + K_{ym}y - \omega_{nm}t + \phi_{nm}$$

and

- K_{xn}, K_{ym} are the physical wavenumbers in the x and y directions, respectively, measured in $[rad/m]$.
- ω_{nm} is the angular frequency in $[rad/sec]$. In the case of infinite depth, and when nonlinearities are not considered, the following dispersion relation holds:

  $$\omega_{nm}^2 = g\sqrt{K_{xn}^2 + K_{ym}^2} = gK_{nm}$$

  with g the gravitational constant in $[m/sec^2]$.
- ϕ_{nm} are independent random phases in $[rad]$ usually assumed to be uniformly distributed in $[-\pi, \pi]$.
- a_{nm} are random amplitudes in $[m]$, such that $a_{nm}\cos\phi_{nm}$ and $a_{nm}\sin\phi_{nm}$ are independent and normally distributed random variables, i.e. a_{nm} is Rayleigh distributed. The Rayleigh parameter is obtained through

  $$\sum_{\forall n | K_n \in \Delta K_x} \sum_{\forall m | K_m \in \Delta K_y} \frac{\overline{a_{nm}^2}}{2} = S(K_x, K_y)\Delta K_x \Delta K_y = \Psi(K,\theta) K \Delta K \Delta\theta = F(\omega,\theta)\Delta\omega\Delta\theta$$

- Finally, the summation orders N and M, simply indicate the fineness of the model approximation.

For a practical implementation (ignoring the time dimension), we start with

$$\zeta(x,y) = \sum_{n=1}^{N}\sum_{m=1}^{M} a_{nm}\cos(K_{xn}x + K_{ym}y + \phi_{nm}) \quad ,$$

which becomes

$$\zeta(x,y) = \sum_{n=1}^{N}\sum_{m=1}^{M} r_{nm}\sqrt{2S(K_{xn},K_{ym})\Delta K_{xn}\Delta K_{ym}}\cos(K_{xn}x + K_{ym}y + \phi_{nm}) \quad , \quad (4)$$

where r_{nm} designates normalized Rayleigh random variables. This equation states that we can sample the spectrum, once, within a $\Delta K_x \Delta K_y$ differential grid element, for each (K_{xn}, K_{ym}) pair and add the contributions. If more spectrum samples are taken within the grid element, two more summations are performed to handle all additional pairs (K_{xni}, K_{ymj}). This is not necessary for a small enough grid.

Some workers make the additional simplification of setting $r_{nm} = 1$, i.e. ignoring the amplitude fluctuations, the reasoning being that, due to the central limit theorem, the original process becomes asymptotically Gaussian and the fluctuations are averaged out. This approach essentially gives a "smoothed" surface description.

Significant computational savings are realized when, instead of performing the summations directly, we do a two-dimensional inverse FFT on the spectrum matrix multiplied term-by-term by a phase matrix factor $\exp(j\phi_{nm})$. For example, for identical results, the direct summation approach can take about six hours for a 512×512 patch, while the FFT approach can be finished in less than a minute.

3.3 Directional Ocean Spectra Examples

The discussion up to this point indicates that knowledge of the sea surface directional spectrum is sufficient to generate Gaussian sea surface patches. Such spectra depend on several factors, among which are weather conditions, geographical location and wind speed. Properties common to all ocean spectra are:

- All measured spectra have an upper limit after which any additional input energy to the wave system from the wind goes to the formation of breaking waves, capillary waves and other secondary phenomena.
- The spectra do not contain any dc components.

- After the peak frequency or peak wavenumber, there is a decay which mainly follows an ω^{-5} or k^{-4} power law.

It should, however, be borne in mind that most spectrum models are usually applicable to equilibrium conditions only and that, in practice, the sea surface conditions often admit non-fully developed spectra and multi-modal wave systems. This is still an active research area.

Due to the difficulty of accurately measuring the full directional spectrum, most models assume that it can be described as the product of a nondirectional spectrum and a spreading function as follows:

$$\Psi(K,\theta) = \psi(K)D(K,\theta) \tag{5}$$

where

$$\psi(K) = \int_{-\pi}^{\pi} \Psi(K,\theta)d\theta = \int_{0}^{2\pi} \Psi(K,\theta)d\theta \quad ,$$

and

$$\int_{-\pi}^{\pi} D(K,\theta)d\theta = \int_{0}^{2\pi} D(K,\theta)d\theta = 1 \quad ,$$

with $D(K,\theta)$ often given in terms of θ alone. Note that this separability assumption should always be used with caution when dealing with real data.

3.3.1 Pierson-Moskowitz Realization

The classic model of a wind generated, wave system is the one developed by Pierson and Moskowitz. An example of sea surface synthesis based on this model is described in [9]. The authors start with the downwind power spectrum for fully developed sea conditions,

$$\Phi(f) = \frac{\alpha g^2}{(2\pi)^4 f^5} \exp\left[-\frac{5}{4}\left(\frac{f_m}{f}\right)^4\right] \quad ,$$

where f is the frequency in Hz, f_m the peak frequency, $\alpha = 0.0081$ is the Phillips constant and g is the gravitational constant. The peak frequency is directly related to the wind speed at a height of 10 m above the sea surface, u_{10}, through

$$f_m = \frac{0.13g}{u_{10}} \quad .$$

A two dimensional spectrum is generated through

$$\Phi(f,\theta) = \Phi(f)D(f,\theta) \quad ,$$

where the spreading factor, suggested by Hasselmann, is defined by

$$D(f,\theta) = \frac{1}{N_p}\cos^{2p}(\theta) \quad ,$$

where

$$p = 9.77\left(\frac{f}{f_m}\right)^{\mu} \quad ,$$

$$\mu = \begin{cases} 4.06 & \text{for} \quad f < f_m \\ -2.34 & \text{for} \quad f > f_m \end{cases}$$

and the normalization constant,

$$N_p = 2^{1-2p}\pi\frac{\Gamma(2p+1)}{\Gamma^2(p+1)} = 2\sqrt{\pi}\frac{\Gamma(p+1/2)}{\Gamma(p+1)} \quad ,$$

is defined such that $\int_{-\pi}^{\pi} D(f,\theta)d\theta = 1$.

Modifying their model by transforming to wavenumber space, allows better control of spatial dimensions. This is done through the dispersion relation, which for simplicity, we take to be linear (appropriate for deep seas), so that

$$\omega^2 = gK \qquad \text{or} \qquad f = \frac{\sqrt{gK}}{2\pi} \quad .$$

The surface height variance is

$$\sigma^2 = \int_{-\infty}^{\infty}\int_{-\infty}^{\infty}\Psi(\mathbf{K})d\mathbf{K} = \int_0^{2\pi}\int_0^{\infty}\Psi(K,\theta)KdKd\theta =$$

$$= \int_0^{\infty}\psi(K)KdK = \int_0^{\infty}\Phi(\omega)d\omega = 2\pi\int_0^{\infty}\Phi(f)df \quad ,$$

where we assume that the separability condition (5) holds. We then obtain the proper spectral relationship

$$\Psi(K) = \frac{2\pi\Phi(f)}{K}\frac{df}{dK} = \frac{\alpha\pi}{K^4}\exp\left[-1.25\left(\frac{K_p}{K}\right)^2\right] \quad ,$$

where

$$K_p = \left[\frac{0.13\times 2\pi}{u_{10}}\right]^2 g \quad .$$

In applying the linear superposition approach with summations performed using a two-dimensional FFT routine, care must be taken that both the spatial and wavenumber element grids are of the proper size. For example, in one dimension, from the Nyquist criterion, we have

$$\Delta x\Delta K_x = \frac{2\pi}{N} \quad ,$$

Table 1: Wind speed and ΔK resolution based on the spatial resolution Δx and the grid size N. Spatial resolution values examined are $\Delta x = 0.1$ m (L-band) and $\Delta x = 0.01$ m (X-band).

u_{10} $[m/s]$	K_p $[rad/m]$	ΔK (L-band)	N (L-band)	ΔK (X-band)	N (X-band) m
2	5.125	1.963	32	2.454	256
5	0.820	0.245	256	0.307	2048
10	0.205	0.061	1024	0.077	8192
15	0.091	0.031	2048	0.038	16384

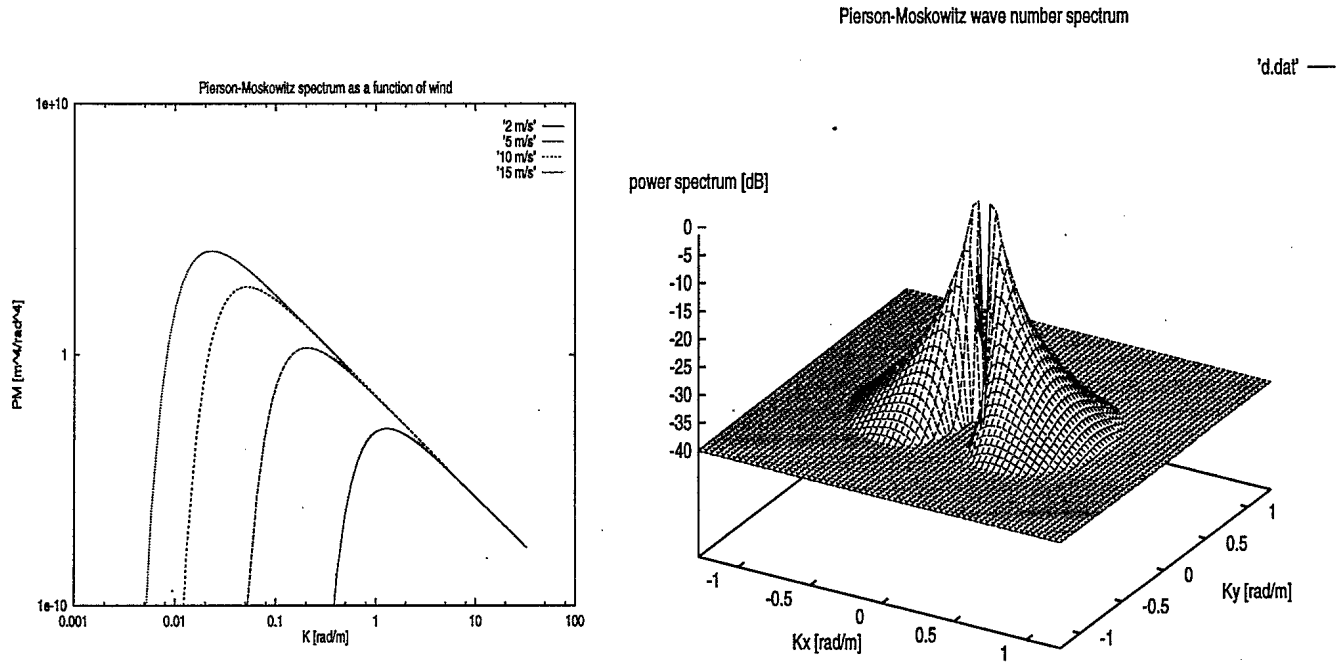

Figure 1: The Pierson-Moskowitz non-directional wavenumber spectrum for $u_{10} = 2$, 5, 10 and 15 m/s on the left, and the directional spectrum for $u_{10} = 10$ m/s on the right.

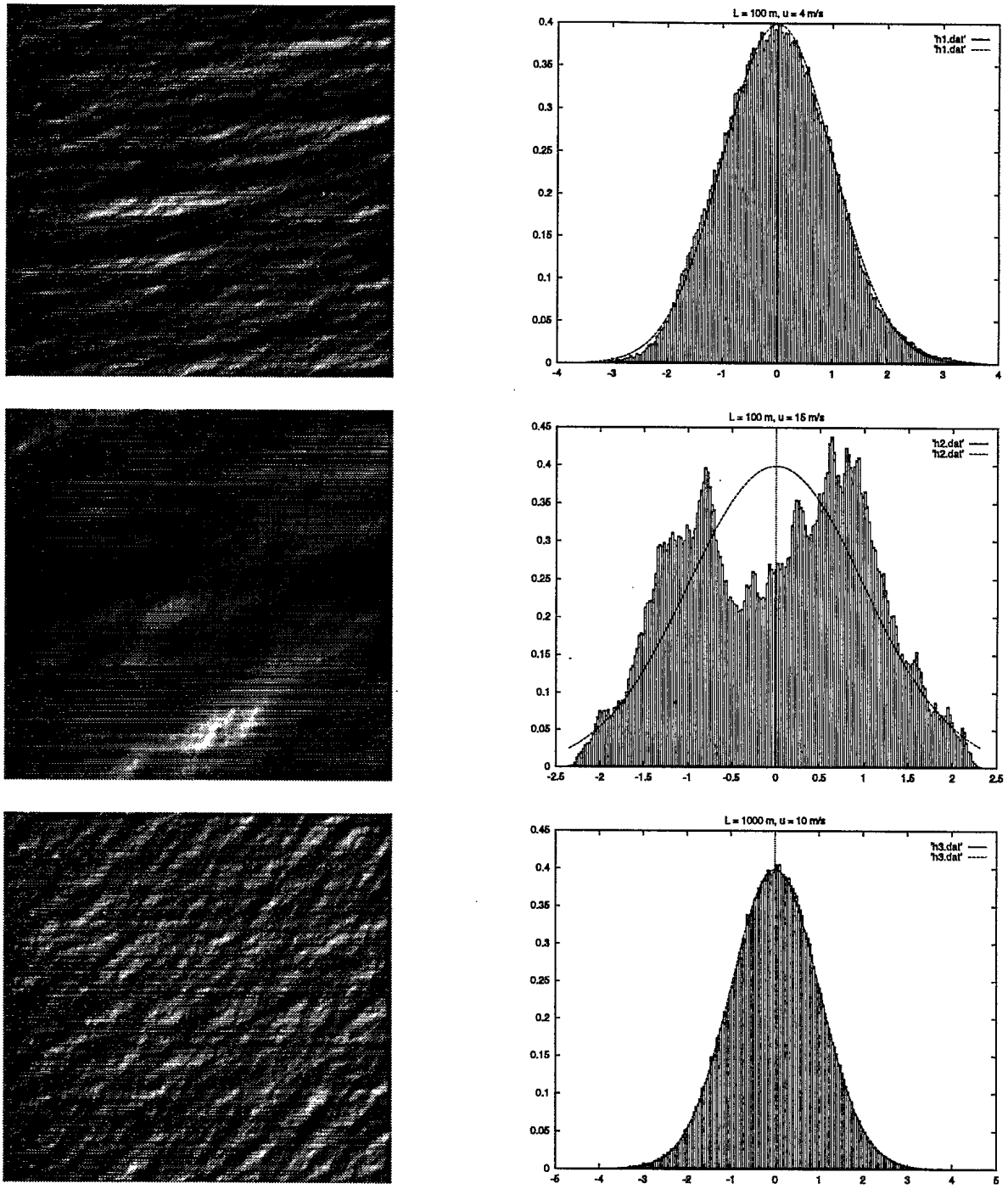

Figure 2: Three surface patches and their histograms based on the Pierson-Moskowitz spectrum. The generating program uses a fixed $N = 512$ and takes as input the patch size L, wind speed u_{10} and wind direction θ_w. From top to bottom: (a) $L = 100$ m, $u_{10} = 4$ m/s, $\theta_w = 0°$, (b) $L = 100$ m, $u_{10} = 15$ m/s, $\theta_w = 0°$, (c) $L = 1000$ m, $u_{10} = 10$ m/s, $\theta_w = 45°$. The image histograms are compared with the Gaussian pdf.

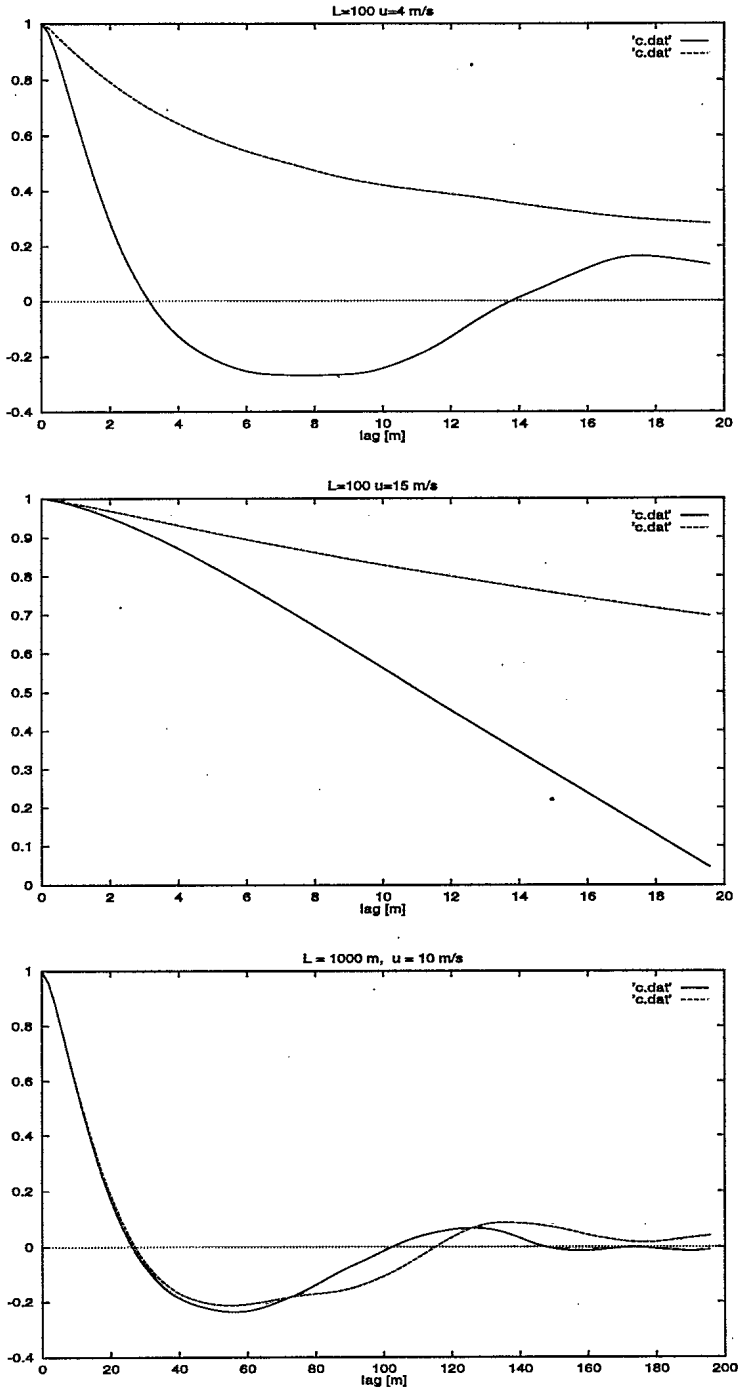

Figure 3: Correlations in the x and y directions of the three cases in Fig. 2. Solid line is x direction, dashed line is y. The wind direction is $\theta_w = 0°$ for the first two graphs and $\theta_w = 45°$ for the third.

where N is the number of grid cells. Holliday [6], based on Bragg scattering considerations, recommends a spatial resolution of $\Delta x = 0.1$ m for L-band and $\Delta x = 0.01$ m for X-band. Given Δx, the number of grid points N must be large enough for adequate **K**-space resolution. The size ΔK must be sufficiently small to properly define the ocean wave spectrum at low wavenumbers. Holliday recommends $\Delta K \sim 0.5K_p$ or less, where K_p is the wavenumber where the spectrum attains its peak.

In the Pierson-Moskowitz model, K_p is inversely proportional to the square of the wind speed at a height of 10 m above sea level, u_{10} (Table 1). The non-directional wavenumber spectrum for some different wind speeds is shown in Fig. 1 together with the directional one for $u_{10} = 10$ m. It is interesting to generate surface patches varying u_{10} and N and look at the patch images and histograms of the surface heights. The image histograms are compared with the Gaussian pdf and Holliday's recommendations are borne out (Fig. 2). The only difference between the first and second patch is the wind speed, from 4 m/s to 15 m/s. This changes the wavenumber resolution for the worse and the histogram reflects this.

It is also of interest to see what the surface autocorrelations look like in the x and y directions for the same three cases (Fig. 3). The x direction corresponds to a wind direction of $\theta_w = 0°$ and the y to $\theta_w = 90°$. For the top graph, where $\theta_w = 0°$, the solid line is along the wind direction and the dashed across. The shape of the autocorrelation function is consistent with a periodic wave structure. The second graph is where the ΔK resolution is not fine enough and in the third graph, at $\theta_w = 45°$, again, the autocorrelation function shape is consistent with a periodic wave structure in both directions.

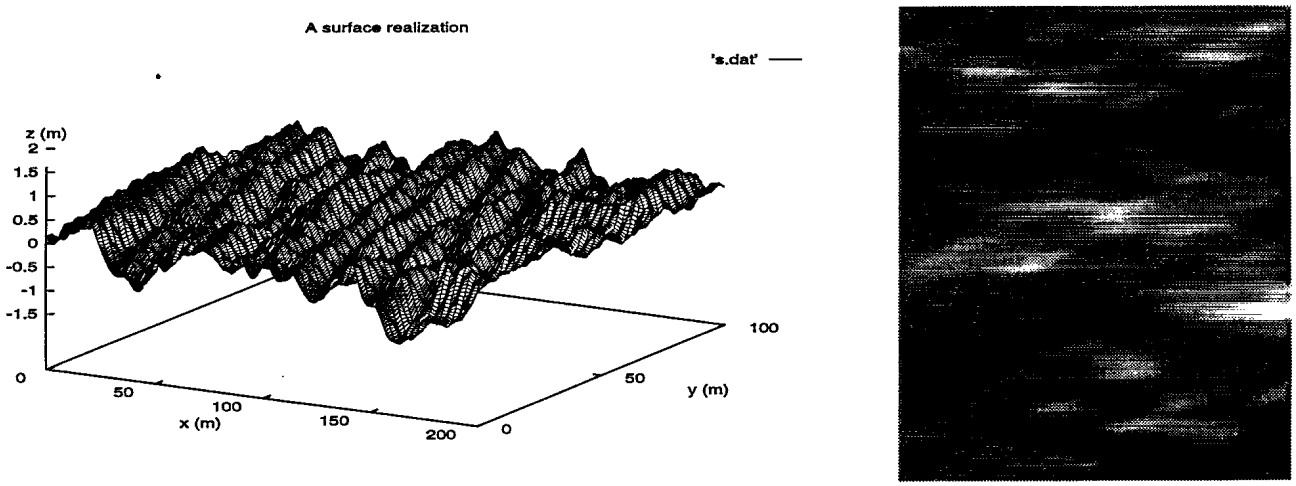

Figure 4: A Trunk surface realization. The surface plot on the left and the grayscale image of the same surface patch on the right.

3.3.2 Trunk's Superposition Model

A variation of the linear superposition approach was used in the past by Trunk [14], employing the parametric equations:

$$x(t) = \delta - \sum_{i=1}^{N} a_i \sin\left[\frac{\omega_i^2}{g}(\delta\cos\theta_i + y\sin\theta_i) - \omega_i t + \gamma_i\right] \quad ,$$

$$y(t) = y \qquad \text{and}$$

$$z(t) = \sum_{i=1}^{N} a_i \cos\left[\frac{\omega_i^2}{g}(\delta\cos\theta_i + y\sin\theta_i) - \omega_i t + \gamma_i\right] \quad ,$$

where (x, y, z) are the coordinates of the sea surface; θ_i is the direction of the ith wave crest, moving with respect to the x-axis and taken from a Gaussian random density with standard deviation 0.5 rad; γ_i are independent uniformly distributed phases between 0 and 2π; and the wave amplitudes a_i are assumed zero-mean Gaussian random variables with variance

$$\sigma^2(a_i) = \frac{1}{N}\int_0^\infty \Phi(\omega)d\omega \quad .$$

The N frequencies ω_i are chosen from

$$\int_0^{\omega_i} \Phi(\omega)d\omega = \frac{2i-1}{2N}\int_0^\infty \Phi(\omega)d\omega$$

and

$$\Phi(\omega) = \frac{dg^2}{\omega^5}\exp\left[-b\left(\frac{g}{u\omega}\right)^4\right]$$

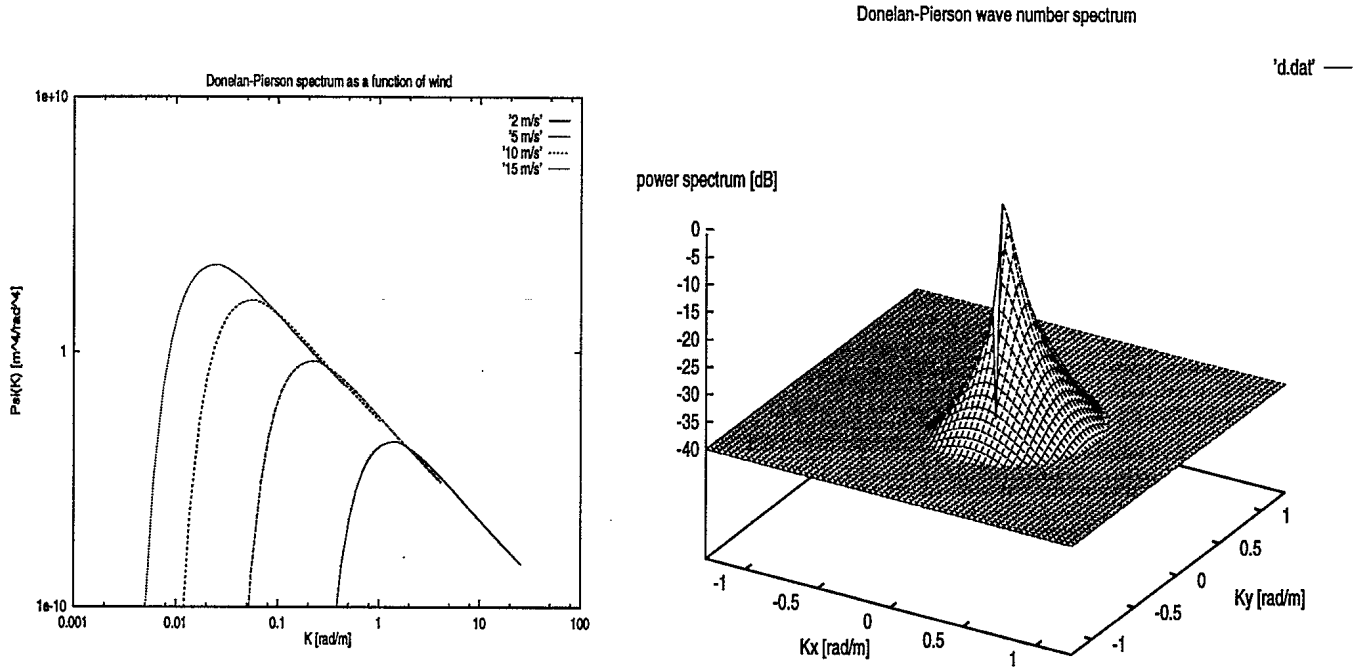

Figure 5: The Donelan-Pierson non-directional wavenumber spectrum for $u_{10} = 2$, 5, 10 and 15 m/s on the left, and the directional spectrum for $u_{10} = 10$ m/s on the right.

where $d = 0.0081$, $b = 0.74$, g is the gravitational constant and u is the windspeed. Allowing the parameter δ to vary from 0 to 200 m with a 0.5 m step size, a realization with $N = 200$ and a 200×100 m patch is generated (Fig. 4).

3.3.3 The Donelan-Pierson Model

A more recent wave number spectrum model, based on exhausting and meticulous experiments, is described in [1]. The low-wave number part is given by

$$\Psi(K,\theta) = \frac{1.62 \times 10^{-3} u_{10}}{K^{3.5}\sqrt{g}} \exp\left(-\frac{K_p^2}{K^2}\right) 1.7^{F(u_{10},K)} h(K/K_p)\mathrm{sech}^2[h(K/K_p)(\theta - \theta_w)]$$

where

$$F(u_{10},K) = \exp\left[-1.22\left(\sqrt{\frac{K}{K_p}} - 1\right)^2\right] \quad ,$$

the spectrum peak is

$$K_p = \frac{g}{(1.2u_{10})^2} \quad ,$$

and the function h is defined as

$$h = \begin{cases} 1.24 & 0 < K/K_p < 0.3 \\ 2.61(K/K_p)^{0.65} & 0.31 < K/K_p < 0.90 \\ 2.28(K_p/K)^{0.65} & 0.90 < K/K_p < 10 \end{cases} \quad .$$

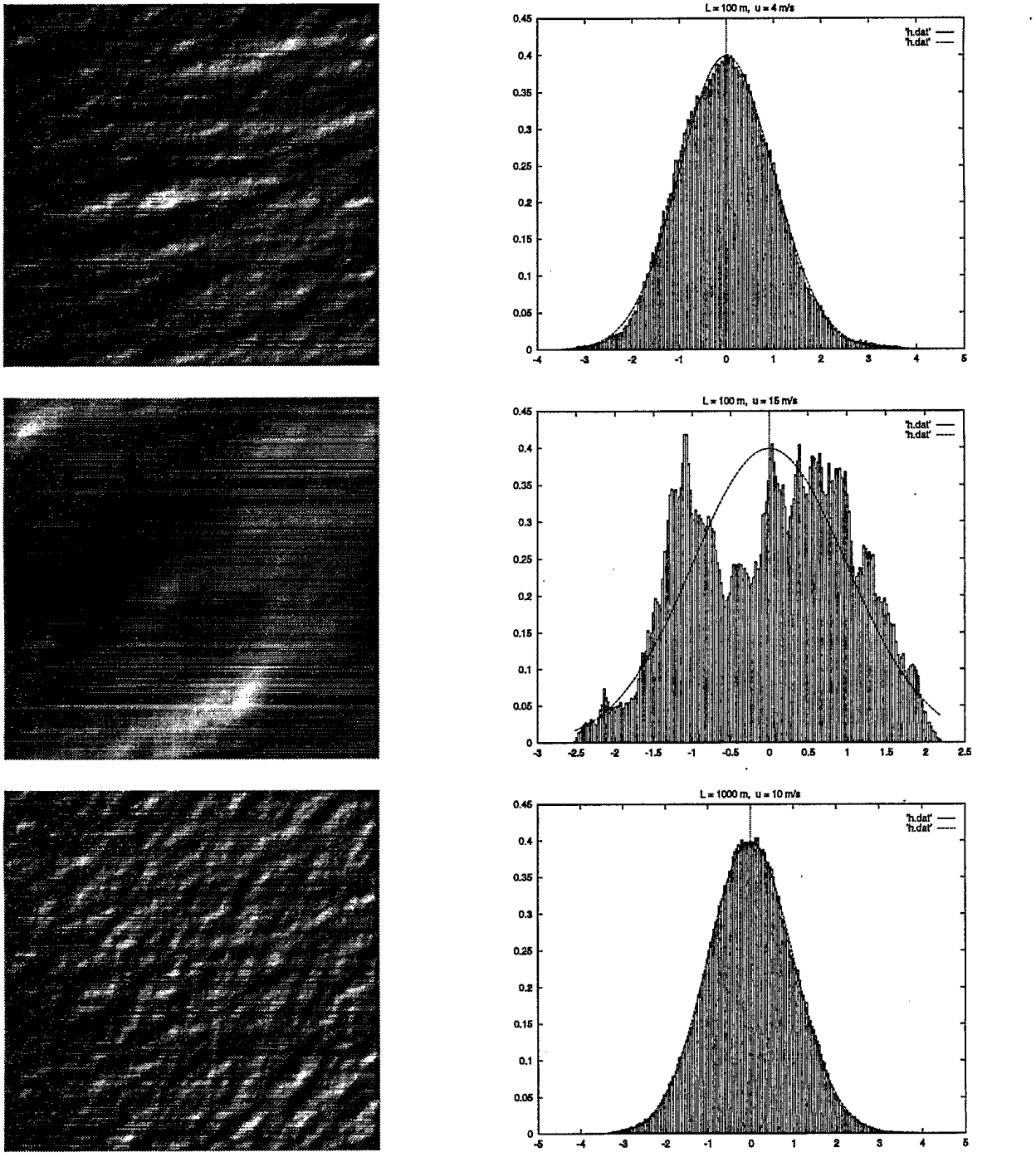

Figure 6: Three surface patches and their histograms based on the Donelan-Pierson spectrum. The generating program uses a fixed $N = 512$ and takes as input the patch size L, wind speed u_{10} and wind direction θ_w. From top to bottom: (a) $L = 100$ m, $u_{10} = 4$ m/s, $\theta_w = 0°$, (b) $L = 100$ m, $u_{10} = 15$ m/s, $\theta_w = 0°$, (c) $L = 1000$ m, $u_{10} = 10$ m/s, $\theta_w = 45°$. The image histograms are compared with the Gaussian pdf.

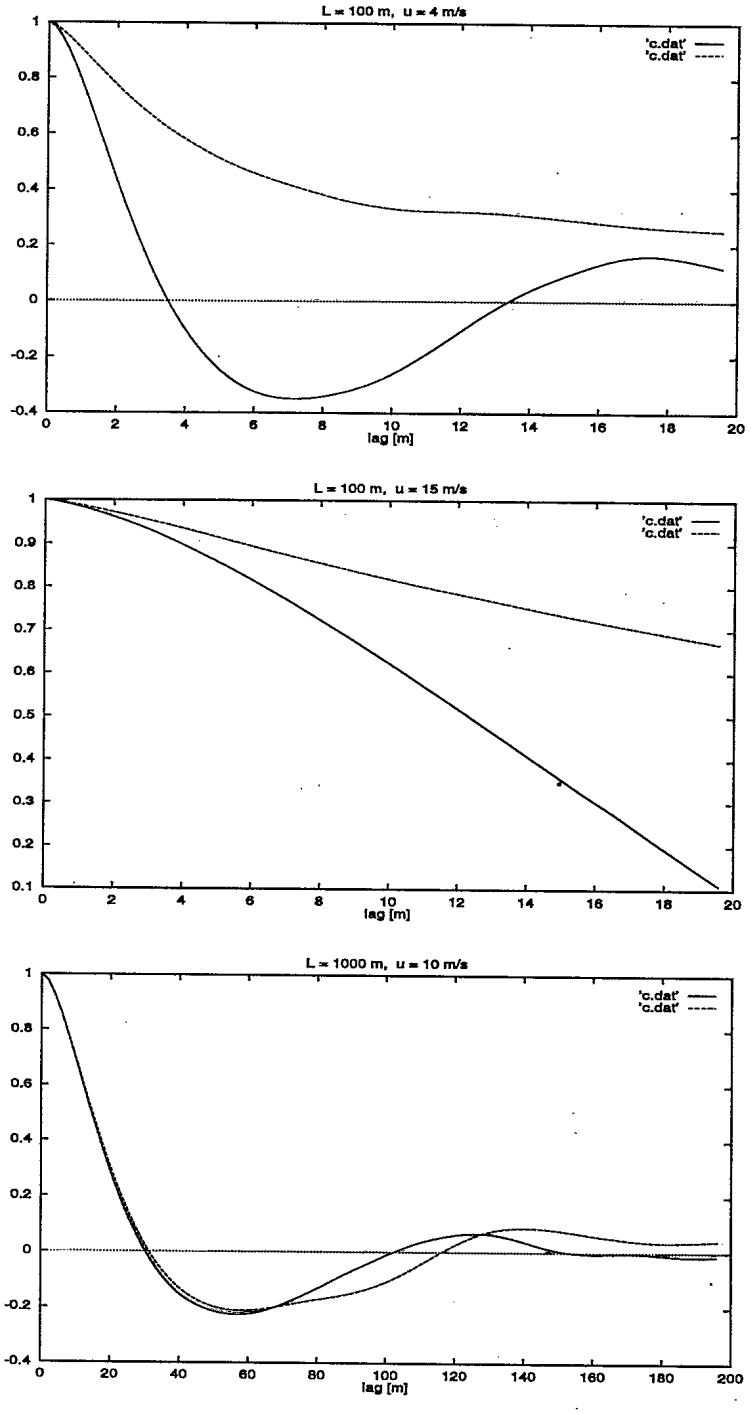

Figure 7: Correlations in the x and y directions of the three cases in Fig. 6. Solid line is x direction, dashed line is y.

This spectrum is considered to be state-of-the-art for an equilibrium, fully-developed sea state. There is also a high wavenumber component, not shown here, that indicates where the drop-off point occurs. From Fig. 5 we see a great deal of similarity with the Pierson-Moskowitz spectrum. The only difference is a shift of the peak to the left and a sharper drop-off to the right. It is the directional component that is significantly different. Note that it is no longer symmetric. The results, however, shown in Fig. 6 and 7 are quite similar to the Pierson-Moskowitz case. Interestingly enough $\Psi(0,0) \neq 0$. This difference is explained in [3] where it is pointed out that the definition used for the sea spectrum, in this development, requires the spectrum to be non-negative for all wave numbers and azimuth angles and to be an integrable function over the wave number and azimuth space.

3.3.4 The Fung and Chen Empirical Spectrum

This last example is of a spectrum that cannot be separated into a polar and directional component [4]. It is instead a single function whose arguments are in terms of $K_x L_x \cos\theta$ and $K_y L_y \sin\theta$, where L_x, L_y are the autocorrelation lengths in the x, y directions, respectively.

The form of this spectrum is

$$\Psi(K,\theta) = \sigma^2 L_x L_y [KA(\theta)][\beta^2 + K^2 A^2(\theta)]^{-3}$$

where

$$\beta = \frac{\pi^{2/3}}{2} \quad \text{, and}$$

$$A(\theta) = \sqrt{(L_x \cos\theta)^2 + (L_y \sin\theta)^2} \quad .$$

Choosing $L_x = 2$ m, $L_y = 3$ m and $\sigma^2 = 1$ we get the results seen in Fig. 8.

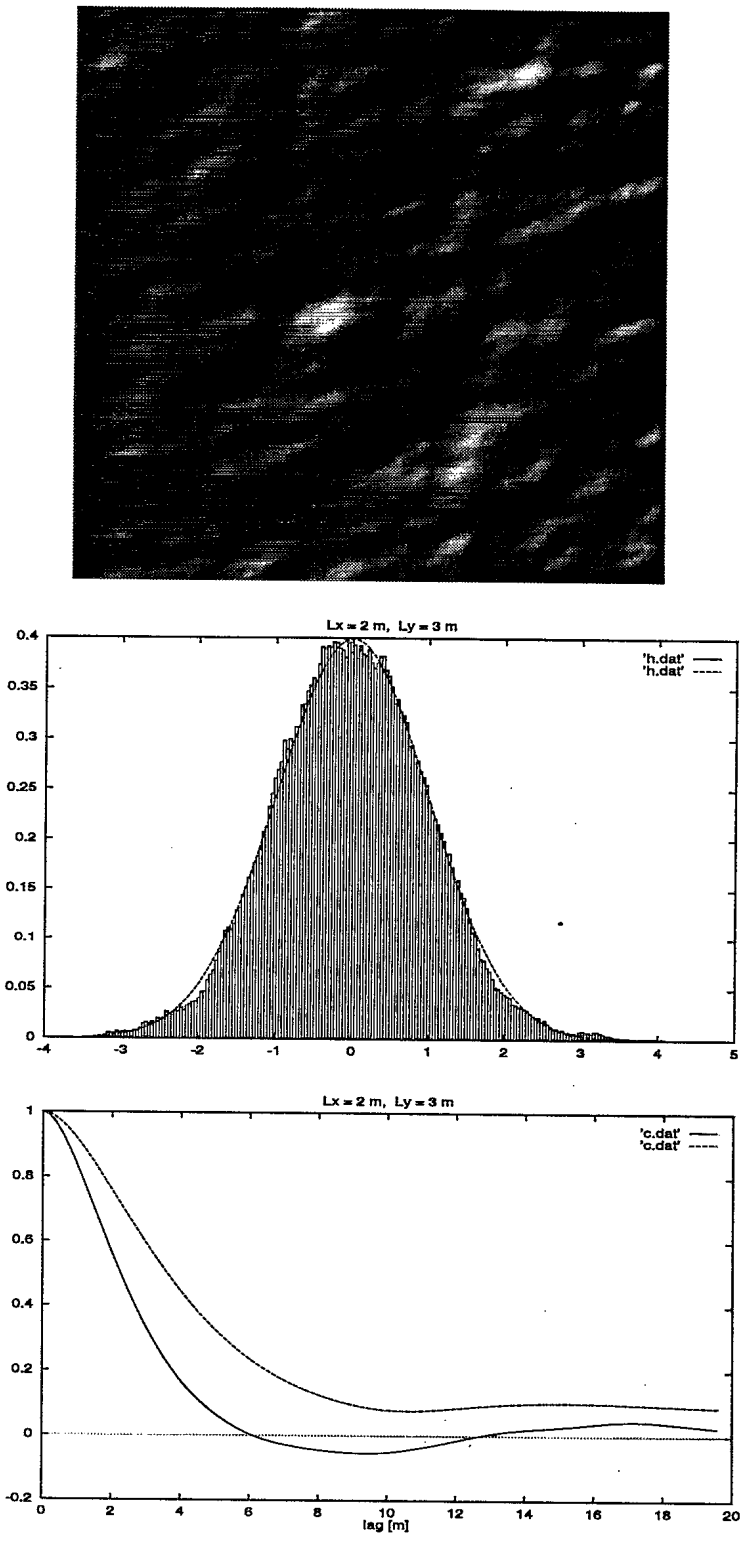

Figure 8: The Fung and Chen empirical spectrum. A surface patch 100×100 m^2, the histogram and the correlations in the x and y directions.

4 Non-Linear Modeling

Oceanographers characterize the sea surface as "weakly non-linear", that is to say the sea surface, to a first approximation, can be represented as a linear sum of independent random components. However, quadratic and higher-order interactions between the components cannot be entirely neglected. Some of the shortcomings of the linear model are:

- Under moderate wind conditions, it is well known that the wave crests are tilted in the upwind direction (skewness).
- It has been reported, experimentally, that the ocean's normalized azimuthal radar cross section signature, σ^0, measured at 180° azimuth is less than at 0°.
- Surf beats, wave breaking and the energy transfer between wave components can only be explained by the nonlinearity of the wave motion.
- The loss of coherence at two points parallel to the direction of wave propagation and the existence of secondary peaks at about, but not quite, harmonic frequencies to the fundamental wave frequency.

The linear approximation, as one would expect, corresponds to the ordinary Gaussian distribution. The higher order approximations can be described by the Gaussian law multiplied by certain polynomials, corresponding in fact, to successive terms in a Gram-Charlier series expansion.

Longuet-Higgins, one of the pioneers in this area, used the cumulant generating function to derive an expression for the pdf of a weakly nonlinear ocean surface [8]. Starting from the moment generating function $\phi(t)$, defined as the Fourier transform of the pdf $f(\zeta)$, where ζ is the sea surface elevation,

$$\phi(t) = \int_{-\infty}^{\infty} f(\zeta) \exp(jt\zeta) d\zeta \quad .$$

The pdf can be written as

$$f(\zeta) = \frac{1}{2\pi} \int_{-\infty}^{\infty} \phi(t) \exp(-j\zeta t) dt = \frac{1}{2\pi} \int_{-\infty}^{\infty} \exp[K(t) - j\zeta t] dt \quad ,$$

where $K(t) = \ln \phi(t)$ is the cumulant generating function. The cumulants are generated from

$$\kappa_k = (-j)^k \frac{\partial^k K(t)}{\partial t^k}|_{t=0}$$

and the moments from

$$m_k = (-j)^k \frac{\partial^k \phi(t)}{\partial t^k}|_{t=0} \quad .$$

The first four cumulants are related to the first four moments through

$$\kappa_1 = m_1$$

$$\kappa_2 = m_2 - m_1^2$$

$$\kappa_3 = m_3 - 3m_1m_2 + 2m_1^3$$

$$\kappa_4 = m_4 - 3m_2^2 - 4m_3m_1 + 12m_2m_1^2 - 6m_1^4 \quad .$$

It can be seen that the first two cumulants are the mean and variance of the process. For nonlinear investigations, the skewness and kurtosis parameters are useful. The first is a measure of pdf asymmetry and the second of pdf flatness. Skewness and kurtosis are defined as

$$\lambda_3 = \frac{\kappa_3}{\kappa_2^{3/2}} \qquad \text{and}$$

$$\lambda_4 = \frac{\kappa_4}{\kappa_2^2}$$

respectively.

Replacing $K(t)$ by its Taylor series expansion, the pdf can be rewritten as

$$f(\zeta) = \frac{1}{2\pi}\int_{-\infty}^{\infty} \exp\left[(\kappa_1 - \zeta)(jt) + \frac{1}{2}\kappa_2(jt)^2 + \frac{1}{6}\kappa_3(jt)^3 + \cdots\right] dt \quad .$$

After performing the change of variables given by

$$x = (\zeta - \kappa_1)/\sqrt{\kappa_2} \qquad \text{and}$$

$$t = s/\sqrt{\kappa_2} \quad ,$$

we have, up to the fourth order moments,

$$f(\zeta) = \frac{1}{2\pi\sqrt{\kappa_2}}\int_{-\infty}^{\infty} \exp\left[-\frac{s^2 + 2jxs}{2}\right] \times \left[1 + \frac{1}{3}\lambda_3(js)^3 + \frac{1}{24}\lambda_4(js)^4 + \cdots\right] ds =$$

$$= \frac{1}{\sqrt{2\pi\kappa_2}} \exp\left(-\frac{x^2}{2}\right) \exp\left[1 + \frac{1}{3}\lambda_3 H_3 + \left(\frac{1}{24}\lambda_4 H_4 + \frac{1}{72}\lambda_3^2 H_6\right) + \cdots\right] \quad ,$$

where H_n is the Hermite polynomial of order n defined by

$$H_n(x) = x^n - \frac{n(n-1)}{1!}\frac{x^{n-2}}{2} + \frac{n(n-1)(n-2)(n-3)}{2!}\frac{x^{n-4}}{2^2} + \cdots \quad .$$

Note that when the higher order moments are neglected, the pdf reduces to its Gaussian form. The higher order terms represent the nonlinearities of the surface distribution.

The sea surface equation can now be written as the superposition of several perturbation orders. The first order is the Gaussian linear model, the second order includes the squares of the amplitudes, the third includes the cubes of the amplitudes, and so on, such that

$$\zeta(x,y,t) = \zeta^{(1)} + \zeta^{(2)} + \zeta^{(3)} + \cdots \quad .$$

To each component $\zeta^{(i)}$ corresponds a velocity potential $\phi^{(i)}$ which, together with $\zeta^{(i)}$, describe the boundary conditions of the surface. Longuet-Higgins solved these boundary conditions [8] for the second order approximation $\zeta^{(2)}$:

$$\begin{aligned}\zeta^{(2)} = \sum_i \sum_j \frac{a_i a_j}{\sqrt{K_i K_j}} \{ & [B_{ij}^- + B_{ij}^+ - \mathbf{K}_i \cdot \mathbf{K}_j \\ & + (K_i + K_j)\sqrt{K_i K_j}] \cos\psi_i \cos\psi_j \\ & + [B_{ij}^- - B_{ij}^+ - K_i K_j] \sin\psi_i \sin\psi_j \}\end{aligned}$$

where

$$B_{ij}^{\pm} = \frac{(\sqrt{K_i} \pm \sqrt{K_j})^2 (\mathbf{K}_i \cdot \mathbf{K}_j \mp K_i K_j)}{(\sqrt{K_i} \pm \sqrt{K_j})^2 - |\mathbf{K}_i \pm \mathbf{K}_j|} \quad .$$

A sea surface realization based on this model would require the computation of $\zeta^{(1)} + \zeta^{(2)}$. Note that the above model is developed for "free" waves in which not only is the viscous damping neglected, but it is also assumed that the stresses at the free surface are identically zero. The atmosphere alone is expected to produce wave asymmetry with the above phenomena as it acts on the sea surface.

Before Longuet-Higgins, Tick [13] followed a similar approach based on third order Stokes waves. Tayfun [11, 12] employed the same principle based on second order Stokes waves to apply his results to narrow band random waves. The concept of a narrow band process is carried over from Rice's communications theory, where a single dominant carrier wave at a fixed frequency is assumed, and the wave amplitude is allowed to vary slightly within a narrow bandwidth centered about the carrier frequency. The applicability of this model is questionable within the wave generating area where sporadic wave breaking and whitecapping occurs and the narrow band assumption fails. However, as waves propagate out, the spectral amplitudes fall below the saturation range and the bandwidth becomes progressively smaller. Tayfun's narrow band model is then applicable and simpler to implement.

In fact, to second order, and expanding Tayfun's one-dimensional development to two dimensions, the model becomes:

$$\zeta = \zeta_1 + \frac{1}{2} < K > \left(\zeta_1^2 - \bar{\zeta}_1^2\right) \quad ,$$

where $< K >$ is the mean wavenumber defined by

$$< K >= \frac{\int K\Psi(K)dK}{\int \Psi(K)dK}$$

and $\Psi(K)$ is the unidirectional spectrum. The ζ_1 component is the linear, Gaussian surface generated as shown in the previous section and $\bar{\zeta}_1$ is its normal. There is another advantage of using the FFT approach in the previous section. The real part of the FFT is ζ_1 and the imaginary part is $\bar{\zeta}_1$. Fig. 9 shows the implementation for a 1.5×1.5 km patch using Fung and Chen's empirical spectrum as the Gaussian component.

Tayfun mentions that his model results in a random surface whose crests are narrow and peaked and whose troughs are long and flat. Such asymmetry is called vertical skewness. On the other hand, horizontal skewness can also occur in deep water waves. The latter asymmetry results in tilted crests, an effect which directly influences the surface slope distribution. A variety of sparse experimental data, over the years, indicates that the slope distribution is more strongly skewed than the surface elevation.

Finally, general observations of interest to radar analysis of sea clutter data are:

- The wave slopes form the dominant contribution to the radar backscattered signal since only when they point in the right direction does a significant reflection occur.
- The resonant scatterers for microwaves are the capillary waves (capillary wavelength $\sim$ microwave wavelength) about whom little is known experimentally except for the fact that they "bunch" more towards the wave peaks and are wind direction dependent. This is an active research area and in the past few years a variety of new techniques for measuring their spectra have been developed.

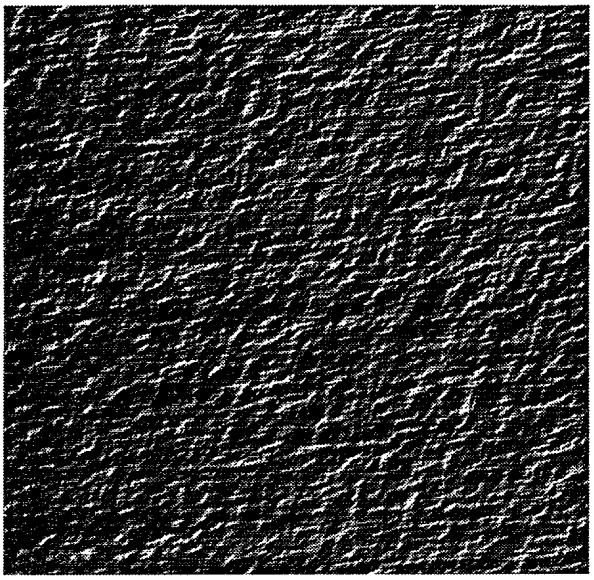

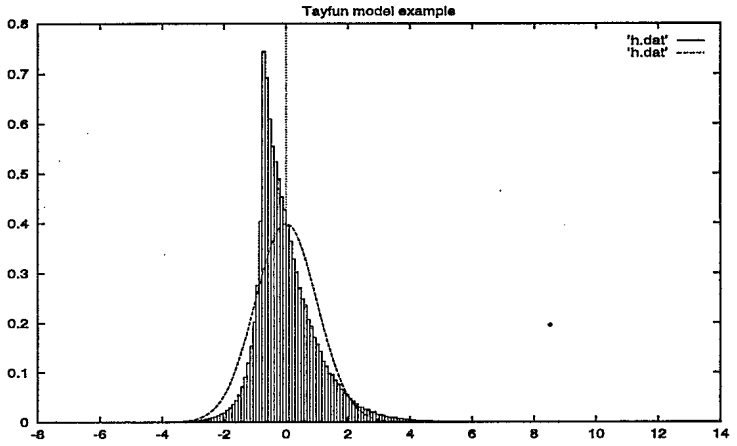

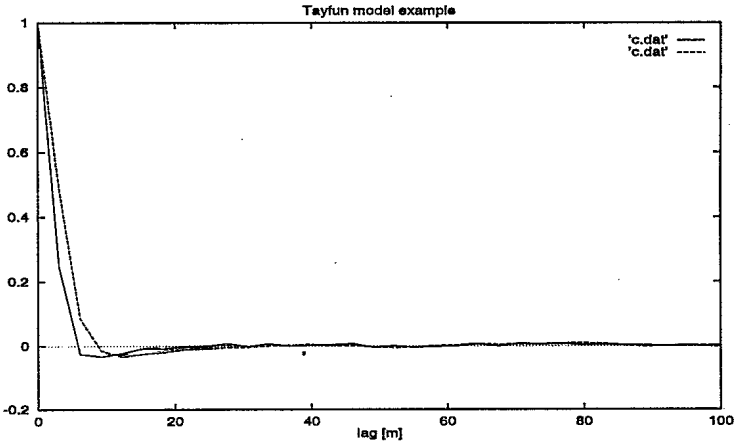

Figure 9: Tayfun's narrow-band nonlinear model for a 1.5×1.5 km patch, the histogram and the correlations in the x and y directions. Note the significant departure from Gaussianity in the histogram.

5 MARCOT Spectra

Some actual experimentally derived wave directional spectra are presented in Fig. 10 for comparison with the previous models and examples. The spectra were estimated from ground-truthed data collected during the MARCOT trials, on June 25 1995. The location was "The Patch", a bank offshore Nova Scotia, in the vicinity of 44°18′41.3″ N 62°18′12.7″ W in waters of approximately 80 m depth. This is an example where the primary sensor used was a common marine radar (MACRADAR) refitted with a TITAN board that allowed data collection directly from the receiver front end, with no dynamic losses due to receiver preprocessing. The PPI images collected with this radar were used to estimate the relative directional wave spectrum according to the method described in [15]. A DATAWELL waverider buoy, a YOUNG wind speed and direction sensor, an air temperature sensor and a Differential Global Positioning System (DGPS) were also deployed. Details of the ground truthing are given in [5].

It is very interesting to observe the time evolution of the spectrum in five minute interval steps under strong, wave development conditions. As time went on, a strong "sea" was developing from two different directions (bimodality of the wave spectrum) and a small craft warning was being broadcast.

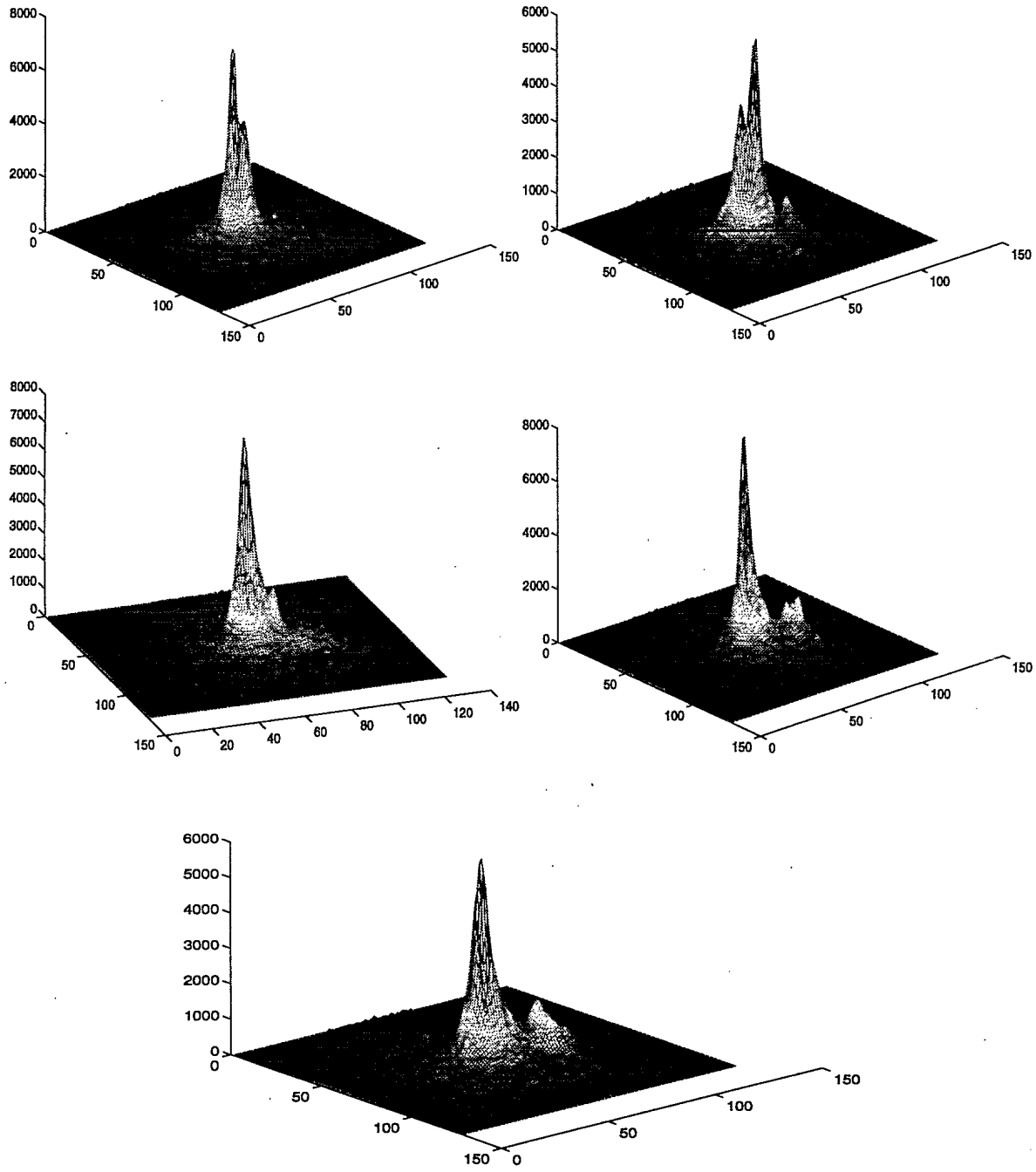

Figure 10: Some of the MARCOT spectra. Top left was at 7:45, top right at 7:50, middle left at 7:55, middle right at 8:00 and bottom one at 8:05. The variability in time and developing bimodality is clearly evident.

6 Conclusion

The framework developed for generating linear Gaussian wave patches is general enough that one can use any theoretical or experimental spectrum as input and generate surface patches of the desired characteristics. These patches can then be used in electromagnetic scattering models to infer accurate sea clutter behavior.

The FFT technique is excellent for application to this purpose as it not only is computationally efficient, it also provides the surface normal, related to the slope distribution, which can be used in some of the simpler nonlinear models. The linear Gaussian model is currently implemented with a two-dimensional FFT that still imposes some memory limitations on the FFT size. This can be improved by more efficient memory allocation, the implementation of the two-dimensional FFT with one-dimensional FFT's or perhaps splitting up the spectrum into short and long wavelength parts, which require a fine and coarse FFT grid respectively, and adding up the results [6].

The nonlinear study is also important as it is here that novel and important effects are expected to appear. Work is currently in progress to implement the full Longuet-Higgins model.

The most important observation however, is, that an equilibrium model is not adequate for the typical case of a non fully developed sea surface. Further work is required in this area and experiments are being planned for an extensive investigation early next year. The non fully developed sea surface conditions are the ones more commonly encountered during radar surveillance operations and should therefore be properly accounted for.

It appears that for radar detection of small targets in sea clutter, there should be an operational mode that estimates the current sea surface spectrum and utilizes this estimate in a way that optimizes target detection. Work is underway in developing such an architecture.

References

[1] M.A. Donelan. Radar Scattering and Equilibrium Ranges in Wind-Generated Waves with Application to Scatterometry. *J. Geophys. Research*, 92(C5):4971–5029, 1987.

[2] M.A. Donelan, J. Hamilton, and W.H. Hui. Directional Spectra of Wind-Generated Waves. *Phil.Trans. R. Soc. Lond. A*, 315:509–562, 1985.

[3] A.K. Fung, K.S. Chen, and M.F. Chen. A Note on the Directional Sea Spectrum. *Remote Sens. Environ.*, 30:95–106, 1989.

[4] A.K. Fung and K.K. Lee. A Semi-empirical Sea Spectrum Model for Scattering Coefficient Estimation. *IEEE J. Oceanic Engineering*, 7:166–176, 1982.

[5] M. Henschel. East Coast Sea Surface Wave Measurements, Contract Report by MacLaren Plansearch, No. 010907RE.001, Sept. 1995.

[6] D. Holliday, G. St-Cyr, and N.E. Woods. A Radar Ocean Imaging Model for Small to Moderate Incidence Angles. *Int. J. Remote Sensing*, 7:1809–1834, 1986.

[7] B. Kinsman. *Wind Waves.* Prentice-Hall, 1965.

[8] M.S. Longuet-Higgins. The Effect of Non-linearities on Statistical Distributions in the Theory of Sea Waves. *J. Fluid Mechanics*, 17:459–480, 1963.

[9] G.A. Mastin, P.A. Watterberg, and J.F. Mareda. Fourier Synthesis of Ocean Waves. *IEEE Computer Graphics and Applications*, pages 16–23, March 1987.

[10] O.M. Phillips. *The Dynamics of the Upper Ocean.* Cambridge University Press, 2nd edition, 1977.

[11] M.A. Tayfun. Narrow-Band Nonlinear Sea Waves. *J. Geophys. Res.*, 85(C5):1548–1552, 1980.

[12] M.A. Tayfun. On Narrow-Band Representation of Ocean Waves; I. Theory. *J. Geophys. Res.*, 91(C6):7743–7752, 1986.

[13] L.J. Tick. A Non-Linear Random Model of Gravity Waves I. *J. of Mathematics and Mechanics*, 8:643–651, 1959.

[14] G.V. Trunk. Non-Rayleigh Sea Clutter: Properties and Detection of Targets. Technical Report 7986, Naval Research Laboratory, 1976.

[15] I.R. Young and W. Rosenthal. A Three-Dimensional Analysis of Marine Radar Images for the Determination of Ocean Wave Directionality and Surface Currents. *J. of Geophys. Res.*, 90(C1):1049–1059, 1985.

UNCLASSIFIED
SECURITY CLASSIFICATION OF FORM
(highest classification of Title, Abstract, Keywords)

DOCUMENT CONTROL DATA

(Security classification of title, body of abstract and indexing annotation must be entered when the overall document is classified)

1. ORIGINATOR (the name and address of the organization preparing the document. Organizations for whom the document was prepared, e.g. Establishment sponsoring a contractor's report, or tasking agency, are entered in section 8.)

Defence Research Establishment Ottawa
Ottawa, ON, K1A 0Z4

2. SECURITY CLASSIFICATION (overall security classification of the document. including special warning terms if applicable)

UNCLASSIFIED

3. TITLE (the complete document title as indicated on the title page. Its classification should be indicated by the appropriate abbreviation (S,C or U) in parentheses after the title.)

Sea Surface Modeling and Simulation (U)

4. AUTHORS (Last name, first name, middle initial)

Drosopoulos, Anastasios

5. DATE OF PUBLICATION (month and year of publication of document)

December 1995

6a. NO. OF PAGES (total containing information. Include Annexes, Appendices, etc.)

39

6b. NO. OF REFS (total cited in document)

15

7. DESCRIPTIVE NOTES (the category of the document, e.g. technical report, technical note or memorandum. If appropriate, enter the type of report, e.g. interim, progress, summary, annual or final. Give the inclusive dates when a specific reporting period is covered.)

Technical Report

8. SPONSORING ACTIVITY (the name of the department project office or laboratory sponsoring the research and development. Include the address.)

9a. PROJECT OR GRANT NO. (if appropriate, the applicable research and development project or grant number under which the document was written. Please specify whether project or grant)

03C03

9b. CONTRACT NO. (if appropriate, the applicable number under which the document was written)

10a. ORIGINATOR'S DOCUMENT NUMBER (the official document number by which the document is identified by the originating activity. This number must be unique to this document.)

DREO REPORT 1282

10b. OTHER DOCUMENT NOS. (Any other numbers which may be assigned this document either by the originator or by the sponsor)

11. DOCUMENT AVAILABILITY (any limitations on further dissemination of the document, other than those imposed by security classification)

(X) Unlimited distribution
( ) Distribution limited to defence departments and defence contractors; further distribution only as approved
( ) Distribution limited to defence departments and Canadian defence contractors; further distribution only as approved
( ) Distribution limited to government departments and agencies; further distribution only as approved
( ) Distribution limited to defence departments; further distribution only as approved
( ) Other (please specify):

12. DOCUMENT ANNOUNCEMENT (any limitation to the bibliographic announcement of this document. This will normally correspond to the Document Availabilty (11). However, where further distribution (beyond the audience specified in 11) is possible, a wider announcement audience may be selected.)

UNCLASSIFIED
SECURITY CLASSIFICATION OF FORM

13. ABSTRACT (a brief and factual summary of the document. It may also appear elsewhere in the body of the document itself. It is highly desirable that the abstract of classified documents be unclassified. Each paragraph of the abstract shall begin with an indication of the security classification of the information in the paragraph (unless the document itself is unclassified) represented as (S), (C), or (U). It is not necessary to include here abstracts in both offical languages unless the text is bilingual).

This report describes the modeling and generation of realistic sea surfaces using state-of-the-art directional wave number spectra. Model details are explained and a preliminary investigation in nonlinear, non-Gaussian aspects is carried out. The surfaces so generated can then be used as input in current radar scattering models to accurately predict sea clutter behavior.

14. KEYWORDS, DESCRIPTORS or IDENTIFIERS (technically meaningful terms or short phrases that characterize a document and could be helpful in cataloguing the document. They should be selected so that no security classification is required. Identifiers, such as equipment model designation, trade name, military project code name, geographic location may also be included. If possible keywords should be selected from a published thesaurus. e.g. Thesaurus of Engineering and Scientific Terms (TEST) and that thesaurus-identified. If it is not possible to select indexing terms which are Unclassified, the classification of each should be indicated as with the title.)

Sea surface modeling, sea clutter modeling, sea surface generation

Sea surface simulation

155034